

# Effects of the Fibroblast-myocyte in Cardiac Electromechanical Coupling: A Preliminary Simulation Study

Heqing Zhan<sup>1</sup>, Ling Xia<sup>1</sup>, Ran Huang<sup>2</sup>

<sup>1</sup> Department of Biomedical Engineering, Zhejiang University, Hangzhou, 310027, China

<sup>2</sup> The Department of Utility Model Examination, State Intellectual Property Office of the People's Republic of China, Beijing, 100086, China

## Abstract

*The heart consists of myocytes, vasculature cells and connective tissue cells. In this study, two ventricular electromechanical models were coupled with the fibroblast model. At the cellular level, Niederer-Smith (NS) model of rat ventricular myocyte and ten Tusscher model of human ventricular myocyte and the passive fibroblast model are combined with Rice model of contraction and cooperativity mechanisms. At the tissue level, excited conduction is integrated with elastic mechanics. Numerically, the finite difference method solves the excitation equations, and the finite element method settles the equations governing tissue mechanics. The results showed that fibroblasts slow down wave propagation and increase mesh contraction. The influence of fibroblasts on cardiac excitation and contraction should be pursued in future heart modeling studies*

## 1. Introduction

Researches on cardiac electrophysiology at the cellular level are very numerous. Along with the development of patch clamp technique and computer, studies based on the model framework developed gradually mature. They were widely used for the diffusion of excitation in tissue and cell-cell interaction (1-3). In mechanical models of myocardial cells, the typical model is Rice model of contraction and cooperativity mechanisms (4). The model exhibits the mechanism of myofilament dynamics clearly and provides complete parameters to describe the process of contraction and relaxation of myocytes. The heart consists of myocytes, vasculature cells and connective tissue cells (5). Recent studies have documented that fibrosis causes cardiomyocyte decoupling, predisposing the tissue to conduction block and reentry (6-8). Effects of fibroblasts on cardiac electrophysiology and mechanics should not be ignored. There are two different electrophysiological models of ventricular fibroblasts: the "passive" model (9) and the "active" model (10).

In this study, two strongly coupled myocardial-

fibroblastic electromechanical models were proposed, which integrated the fibroblast model with the myocardial electrophysiological model and mechanical model at cellular level, excitation conduction and elastic mechanics at tissue level. To realize the cellular electromechanical coupling, the calcium buffer was introduced in ten Tusscher model. With the proposed model, the effects of fibroblasts on cardiac excitation conduction and contraction were investigated in normal and pathological situations.

## 2. Materials and methods

### 2.1. Cellular electromechanical coupling model

Two cellular models were used here, ten Tusscher model of human ventricular myocyte(11) and the Niederer-Smith (NS) model of rat ventricular myocyte (12). One remarkable thing is that, ten Tusscher model is cellular electrophysiological model, while the NS model is cellular electromechanical coupling model. In order to be coupled with cellular mechanical model (Rice model), we rewrite the equation of the concentration of  $Ca^{2+}$  by adding  $Ca^{2+}$  buffers to  $Ca^{2+}$  dynamics to achieve cellular electromechanical coupling. The equations of  $Ca^{2+}$  buffers are given by:

$$\begin{aligned} \frac{dCmndn_{Ca}}{dt} &= \alpha_{cndn} (Cmndn_{tot} - Cmndn_{Ca}) Ca_i - \beta_{cndn} Cmndn_{Ca} \\ \frac{dTrpn_{Ca}}{dt} &= \alpha_{trpn} (Trpn_{tot} - Trpn_{Ca}) Ca_i - \beta_{trpn} \left[ \frac{1 + 2(1 - Force_{norm})}{3} \right] Trpn_{Ca} \end{aligned} \quad (1)$$

In this way, the equation of the concentration of  $Ca^{2+}$  in the ten Tusscher model turns into,

$$\begin{aligned} \frac{dCa_i}{dt} &= k_0 \cdot Ca_{i_{buf}} (i_{leak} - i_{up} + i_{rel} - \frac{i_{CaL} + i_{bCa} + i_{pCa} - 2i_{NaCa}}{2V_c F} C_m) \\ &\quad - \frac{dCmndn_{Ca}}{dt} - \frac{dTrpn_{Ca}}{dt} \end{aligned} \quad (2)$$

where  $k_0=24.6$ . Thus it can be related to equations of mechanics.

## 2.2. Passive model of cardiac fibroblast

The cardiac fibroblast models have two types, the passive model (9) and the active model (10). Here we use the passive model, that is,

$$I_f = G_f(V_f - E_f) \quad (3)$$

where  $I_f$  is the current of fibroblast,  $V_f$  is the membrane potential of fibroblast,  $G_f$  is the membrane conductance and  $E_f$  is the reversal potential. According to experiments,  $G_f$  ranges from 0.1 to 4 nS (13), and  $E_f$  ranges from -50 to 0 mV(14-18). In this study, we use  $G_f=0.5nS$ ,  $E_f=-20mV$ .

## 2.3. Mechanical model of cardiac myocyte

In this study, Rice mechanical model of cardiac muscle (4, 19) was chosen to be coupled with ten Tusscher model. The present study is mainly investigate the impact of fibroblast on cardiac contraction, we therefore chose the typical mechanical model (4) to represent the force generation in cardiac myofilament.

## 2.4. Fibroblast-myocyte coupling

According to (9), equations of the myocyte-fibroblast coupling model are defined by:

$$C \frac{dV}{dt} = -I_{ion} + \sum_{k=1}^n G_{gap}^k (V^k - V) \quad (4)$$

where  $C$  is  $C_m$  or  $C_f$ ,  $I_{ion}$  is  $I_m$  or  $I_f$ ,  $n$  is the number of coupled neighbors (either myocytes or fibroblasts), and  $G_{gap}^k$  is the gap junction conductance between a cell (either a myocyte or a fibroblast) and its  $k^{th}$  neighbor (either a myocyte or a fibroblast) (9). Based on experiments, it was recorded that  $C_f$  ranges from 6.3 to 75pF (10, 20),  $G_{gap}$  ranges from 0.3 to 8nS in cultured cells (15). Here we use  $C_f=50pF$ ,  $G_{gap}=0.6nS$ .

## 2.5. Cardiac tissue mechanics

We present briefly the formulae according to (21) including stress equilibrium, the finite element approximations and the uniform isotonic boundary loads. The formulae were written as,

$$\begin{aligned} \frac{\partial}{\partial X_M} (T^{MN} F_N^j) &= 0 \\ T^{MN} &= \frac{1}{2} \left( \frac{\partial W}{\partial E_{MN}} + \frac{\partial W}{\partial E_{NM}} \right) + T_a C^{MN} \quad (5) \\ \int_{V_0} T^{MN} F_N^j \frac{\partial \Psi_n}{\partial X_M} dV_0 &= f_n^j \\ f_n^j &= \int_{S_2} p \Psi_n n_j ds \end{aligned}$$

where  $\{X_m\}$  are material coordinates,  $T^{MN}$  is the second Piola-Kirchhoff stress tensor of finite elasticity theory,  $F_N^j$  is the deformation gradient tensor,  $W$  is a scalar strain energy density function,  $E_{MN}$  is Green's strain components,  $C_{MN}$  are components of the contravariant

metric tensor,  $\Psi_n$  are the geometric interpolation functions,  $V_0$  is the undeformed volume,  $S_2$  is the portion of the boundry subject to external tractions,  $F_n^j$  are the external nodal traction forces,  $n_j$  are the coordinates of a vector normal to the boundry,  $p$  is the uniform load. The boundry conditions in the two-dimensional (2D) model are two main types. The central node and the edge nodes were completely fixed in space to prevent rigid-body translations.

Since the mechanical properties of fibroblasts have not been well studied so far, and the flexibility of the heart fibrous connective tissue is poor (22), we assume that all the mechanical grid nodes containing fibroblasts to be fixed in space.

The basic process of models calculation is as follows: All derivatives in equations of myocardial cells and fibroblasts are evaluated using finite difference approximations. Following each time integration step, all parameters of these cells are updated,  $T_a$  are interpolated at finite element Gauss points. Stresses of these active Gauss points serve as inputs to govern the tissue mechanics model. Non-linear Newton iterations are used to solve the stress equilibrium equations. Deformation tensors are then updated to govern equations of the electrical conduction.

In this study, we considered isotropic conduction. The 2D model parameters are the following: finite difference approximations are computed using a time integration step of  $\Delta t=0.01ms$  (millisecond) and a space integration step of  $\Delta x=\Delta y=0.1mm$ (millimeter). The mechanics mesh is defined containing  $11 \times 11$  finite elements. Each mechanical element includes  $7 \times 7$  electrical grid points. Thus, the whole area has  $61 \times 61$  grid points and the distance between every two elements is 0.6mm. The time integration step of mechanics is 2ms. Full details of the model are given in (21).

## 3. Results

### 3.1. Electromechanical coupling at cellular level

Figure 1(a) shows the electromechanical coupling of NS model, which has no plateau phase and notch. Figure 1(b) shows an AP and force generated by Tusscher and Rice coupling model. According to the modified calcium transient, the active stress  $T_a$  is calculated. The resting potential is -86.2mV, maximum plateau potential is 19.0mV,  $V_{max}=361mV/ms$ , and maximum force is 0.02kPa.

Figure 2 shows the effect of coupling three passive fibroblasts to a ventricular myocyte with a  $G_{gap}=20nS$ .  $G_{gap}$  ranges from 0 to 100nS in modeling studies (10, 23-24). In contrast to Figure 1, coupling passive fibroblasts to the simulated myocyte lengthened the ventricular APD (90% repolarization) from 193ms to 227ms, and the peak of the AP is decreased from 36.0mV to 26.8mV.

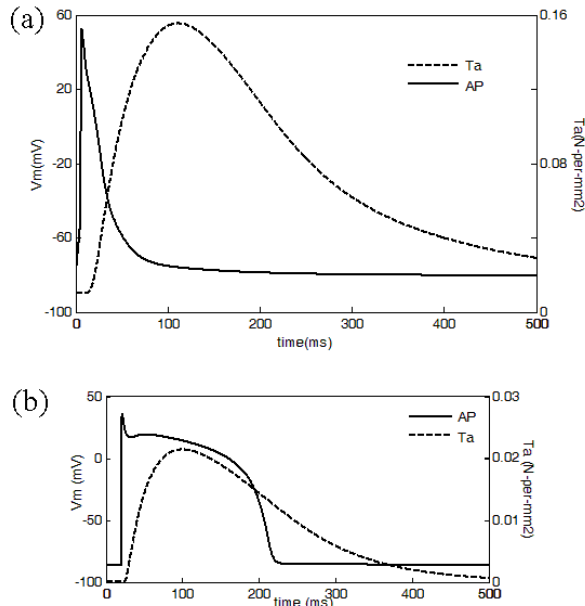


Figure 1. Active potential ( $V$ ) and active stress ( $T_a$ ) generated by the proposed electromechanical coupling model. (a) NS model, (b) ten Tusscher and Rice coupling model.

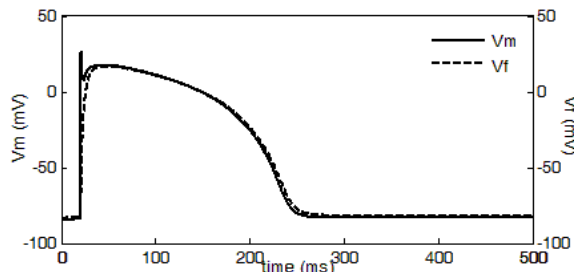


Figure 2. Active potential of myocyte ( $V_m$ ) and fibroblast ( $V_f$ ) after coupling.

### 3.2. Point stimulus in 2D cardiac tissue

Figure 3 shows the effects of central point stimulus on 2D human(a) and rat(b)cardiac tissue. Each top line has no fibroblast and each bottom line has three areas of fibroblasts, distributed as the upper right( $2 \times 2$  finite elements, including  $13 \times 13$  grid points), the lower right ( $2 \times 2$  finite elements, including  $13 \times 13$  grid points) of the central point and the mid left( $4 \times 2$  finite elements, including  $31 \times 13$  grid points), respectively. Stimulate period is 250ms and 100ms.

From Figure 3(a) and (b), we can see that the propagation of excitation wave on the bottom line is slower than that on the top line. In a pure myocyte sheet without fibroblasts, the activation front is circular under isotropic conduction, while in the complex sheet it is deformed. Besides, Contraction around fibroblast areas is obvious. This means fibroblasts reduce conduction

velocity and aggravate contraction.

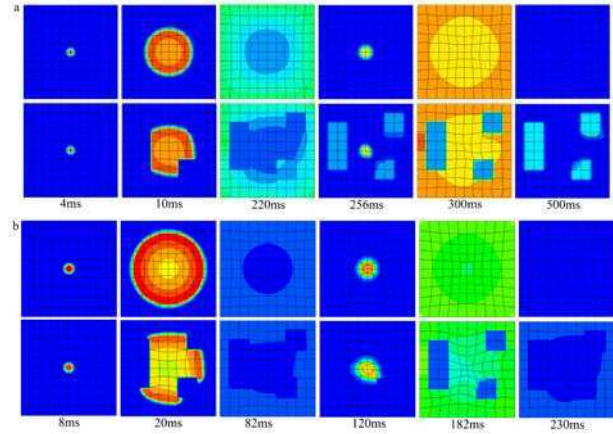


Figure 3. Electromechanical coupling in human (a) and rat (b) cardiac tissue. No fibroblast on each top line and three areas of fibroblasts on each bottom line.

### 4. Discussion

In this study, we present a 2D electromechanical model composed of cardiac myocytes and fibroblasts to investigate effects of fibroblasts on cardiac excitation and contraction. The present study adds fibroblasts to the 2D electromechanical model to reflect more realistic mechanisms of heart and explore possible influences of fibroblasts on cardiac electrophysiology and mechanics.

The results show that fibroblasts may reduce conduction velocity and aggravate contraction. In this study, we use material electrophysiological and mechanical models of cardiac muscles rather than simplified formula and have considered properties of fibroblasts to improve the authenticity of simulation.

Except above results, this study also has some limiting assumptions. Firstly, conduction in myocytes and fibroblasts in this model is set to be isotropic. Secondly, only fibroblast is considered as the mechanism of electromechanical coupling. The other two, stretch activated ionic channels and second messengers/ $Ca^{2+}$  handling in cardiomyocytes are not considered. Finally, the mechanisms of fibroblast mechanics deserve further study. Researches on fibroblast mechanics are mainly on the basis of experiments (22). In this simulation, we consider that when the fibroblast points reach to a certain number, the elasticity of the fibroblasts area will drop rapidly. Therefore, the grids of mechanical elements in the fibroblasts area are set to be fixed. In this assumption, fibroblasts can only concentrate in one region, rather than random distribution. If a handful of fibroblasts are distributed randomly to the mesh grid, the element still has some flexibility, and the grid should not be supposed as fixed. If the detailed model of fibroblast mechanics has been fully worked out, it can be coupled to the myocyte mechanics model to simulate the more precise mechanisms of cardiac electromechanical coupling.

## 5. Summary

In conclusion, we have used two composite models to show real heart tissues. The simulation results suggest that fibroblasts will slow down wave propagation and increase mesh contraction. The effect prove that fibroblasts is a key mechanism in electromechanical coupling and should be valued in cardiac electromechanical modeling.

## Acknowledgements

This project is supported by the 973 National Basic Research & Development Program (2007CB512100), the National Natural Science Foundation of China (30570484) and China Postdoctoral Science Foundation (20090461376).

## References

- [1] Wilders R. Computer modelling of the sinoatrial node. *Med Biol Eng Comput.* 2007 Feb;45(2):189-207.
- [2] Nerbonne JM, Kass RS. Molecular physiology of cardiac repolarization. *Physiol Rev.* 2005 Oct;85(4):1205-53.
- [3] Grandi E, Pasqualini FS, Bers DM. A novel computational model of the human ventricular action potential and Ca transient. *J Mol Cell Cardiol.* 2010 Jan;48(1):112-21.
- [4] Rice JJ, Winslow RL, Hunter WC. Comparison of putative cooperative mechanisms in cardiac muscle: length dependence and dynamic responses. *Am J Physiol.* 1999 May;276(5 Pt 2):H1734-54.
- [5] Manabe I, Shindo T, Nagai R. Gene expression in fibroblasts and fibrosis: involvement in cardiac hypertrophy. *Circ Res.* 2002 Dec 13;91(12):1103-13.
- [6] Xie Y, Garfinkel A, Camelliti P, Kohl P, Weiss JN, Qu Z. Effects of fibroblast-myocyte coupling on cardiac conduction and vulnerability to reentry: A computational study. *Heart Rhythm.* [doi: DOI: 10.1016/j.hrthm.2009.08.003]. 2009;6(11):1641-9.
- [7] de Bakker JM, van Rijen HM. Continuous and discontinuous propagation in heart muscle. *J Cardiovasc Electrophysiol.* 2006 May;17(5):567-73.
- [8] Spach MS, Heidlage JF, Dolber PC, Barr RC. Mechanism of origin of conduction disturbances in aging human atrial bundles: experimental and model study. *Heart Rhythm.* 2007 Feb;4(2):175-85.
- [9] Xie Y, Garfinkel A, Weiss JN, Qu Z. Cardiac alternans induced by fibroblast-myocyte coupling: mechanistic insights from computational models. *Am J Physiol Heart Circ Physiol.* 2009 Aug;297(2):H775-84.
- [10] MacCannell KA, Bazzazi H, Chilton L, Shibukawa Y, Clark RB, Giles WR. A mathematical model of electrotonic interactions between ventricular myocytes and fibroblasts. *Biophys J.* 2007 Jun 1;92(11):4121-32.
- [11] ten Tusscher KH, Noble D, Noble PJ, Panfilov AV. A model for human ventricular tissue. *Am J Physiol Heart Circ Physiol.* 2004 Apr;286(4):H1573-89.
- [12] Niederer SA, Smith NP. An improved numerical method for strong coupling of excitation and contraction models in the heart. *Prog Biophys Mol Biol.* 2008 Jan-Apr;96(1-3):90-111.
- [13] Kohl P, Kamkin AG, Kiseleva IS, Noble D. Mechanosensitive fibroblasts in the sino-atrial node region of rat heart: interaction with cardiomyocytes and possible role. *Exp Physiol.* 1994 Nov;79(6):943-56.
- [14] Camelliti P, Borg TK, Kohl P. Structural and functional characterisation of cardiac fibroblasts. *Cardiovasc Res.* 2005 Jan 1;65(1):40-51.
- [15] Rook MB, Vanginneken ACG, Dejonge B, Elaoumari A, Gros D, Jongsma HJ. Differences in Gap Junction Channels between Cardiac Myocytes, Fibroblasts, and Heterologous Pairs. *American Journal of Physiology.* 1992 Nov;263(5):C959-C77.
- [16] Hyde A, Blondel B, Matter A, Cheneval JP, Filloux B, Girardier L. Homo- and heterocellular junctions in cell cultures: an electrophysiological and morphological study. *Prog Brain Res.* 1969;31:283-311.
- [17] Kohl P. Heterogeneous cell coupling in the heart: an electrophysiological role for fibroblasts. *Circ Res.* 2003 Sep 5;93(5):381-3.
- [18] Kamkin A, Kiseleva I, Wagner KD, Lammerich A, Bohm J, Persson PB, et al. Mechanically induced potentials in fibroblasts from human right atrium. *Exp Physiol.* 1999 Mar;84(2):347-56.
- [19] Iribe G, Kohl P, Noble D. Modulatory effect of calmodulin-dependent kinase II (CaMKII) on sarcoplasmic reticulum Ca<sup>2+</sup> handling and interval-force relations: a modelling study. *Philos Transact A Math Phys Eng Sci.* 2006 May 15;364(1842):1107-33.
- [20] Vasquez C, Moreno AP, Berbari E. Modeling fibroblast-mediated conduction in the ventricle. *Computers in Cardiology 2004, Vol 31.* 2004;31:349-52
- [21] Nash MP, Panfilov AV. Electromechanical model of excitable tissue to study reentrant cardiac arrhythmias. *Prog Biophys Mol Biol.* 2004 Jun-Jul;85(2-3):501-22.
- [22] Brown RA, Prajapati R, McGrouther DA, Yannas IV, Eastwood M. Tensional homeostasis in dermal fibroblasts: mechanical responses to mechanical loading in three-dimensional substrates. *J Cell Physiol.* 1998 Jun;175(3):323-32.
- [23] Jacquemet V, Henriquez CS. Loading effect of fibroblast-myocyte coupling on resting potential, impulse propagation, and repolarization: insights from a microstructure model. *Am J Physiol-Heart C.* 2008 May;294(5):H2040-H52.
- [24] Sachse FB, Moreno AP, Abildskov JA. Electrophysiological modeling of fibroblasts and their interaction with myocytes. *Ann Biomed Eng.* 2008 Jan;36(1):41-56.

Address for correspondence.

Ling Xia  
Department of Biomedical Engineering, Zhejiang University,  
Hangzhou 310027, China  
E-mail: [xialing@zju.edu.cn](mailto:xialing@zju.edu.cn)